

Showcasing joint research from Pohang University of Science and Technology (POSTECH), Republic of Korea, and Tokyo Institute of Technology (TIT), Japan.

Selective dual-purpose photocatalysis for simultaneous  $H_2$  evolution and mineralization of organic compounds enabled by a  $Cr_2O_3$  barrier layer coated on  $Rh/SrTiO_3$

Dual-purpose photocatalysis for  $H_2$  evolution with the simultaneous mineralization of 4-chlorophenol can be achieved under de-aerated conditions using a  $Cr_2O_3/Rh/SrTiO_3$  photocatalyst, which has Rh nanoparticles covered by a thin  $Cr_2O_3$  barrier layer to selectively control the dual-function surface redox reactions.

### As featured in:



See Wonyong Choi et al.,  
*Chem. Commun.*, 2016, **52**, 9636.



Cite this: *Chem. Commun.*, 2016, 52, 9636

Received 20th May 2016,  
Accepted 28th June 2016

DOI: 10.1039/c6cc04260k

[www.rsc.org/chemcomm](http://www.rsc.org/chemcomm)

**Dual-functional photocatalysis for H<sub>2</sub> evolution with the simultaneous mineralization of 4-chlorophenol was achieved under de-aerated conditions using a Cr<sub>2</sub>O<sub>3</sub>/Rh/SrTiO<sub>3</sub> photocatalyst which has Rh nanoparticles covered with a thin Cr<sub>2</sub>O<sub>3</sub> barrier layer to selectively control and maximize the dual-functional photocatalytic activity.**

Hydrogen is considered as an ideal energy storage medium and a promising energy carrier since it can be obtained from abundant natural resources such as water and biomass instead of fossil fuels.<sup>1–4</sup> In particular, photocatalytic water splitting is widely studied as a promising technology to produce hydrogen using solar light.<sup>5–7</sup> Another important application of photocatalysis is the degradation of organic compounds for the remediation of polluted water and air.<sup>8–12</sup> In photocatalytic H<sub>2</sub> production, organic electron donors are commonly used as sacrificial agents to scavenge photogenerated holes.<sup>13–17</sup> However, the intentional addition of organic electron donors (e.g., alcohols, organic acids, amines) for H<sub>2</sub> production is not practically acceptable since the electron donors themselves are another energy resource (often more expensive than H<sub>2</sub>). Therefore, a more desirable strategy is to use organic waste and pollutants in water as *in situ* electron donors. This is the concept of dual-functional photocatalysis which produces H<sub>2</sub> along with the simultaneous degradation of organic pollutants.<sup>18–20</sup> Recently, Kim *et al.* demonstrated that the simultaneous H<sub>2</sub> production with the anoxic photocatalytic degradation of organic compounds can be achieved by using TiO<sub>2</sub> modified by both surface fluorination and Pt deposition (F-TiO<sub>2</sub>/Pt).<sup>19,20</sup>

## Selective dual-purpose photocatalysis for simultaneous H<sub>2</sub> evolution and mineralization of organic compounds enabled by a Cr<sub>2</sub>O<sub>3</sub> barrier layer coated on Rh/SrTiO<sub>3</sub>†

Young-Jin Cho,<sup>a</sup> Gun-hee Moon,<sup>a</sup> Tomoki Kanazawa,<sup>b</sup> Kazuhiko Maeda<sup>b</sup> and Wonyong Choi<sup>a\*</sup>

However, the total organic carbon (TOC) removal efficiency was negligible and TOC remained almost unchanged during the photocatalytic degradation of 4-chlorophenol (4-CP) on F-TiO<sub>2</sub>/Pt, because dioxygen was needed for mineralization. Meeting the optimal condition for dual-purpose photocatalysis is contradictory because the H<sub>2</sub> evolution requires anoxic conditions whereas the mineralization of organic compounds needs dioxygen.

In this study, a selective dual-purpose photocatalysis that achieves H<sub>2</sub> production and TOC removal simultaneously under anoxic conditions is reported. Instead of using the combination of TiO<sub>2</sub> (as a base photocatalyst) and Pt (as a cocatalyst for H<sub>2</sub> evolution), SrTiO<sub>3</sub> (base photocatalyst) and Rh@Cr<sub>2</sub>O<sub>3</sub> core–shell nanostructure (cocatalyst) were employed in this work. The photocatalytic activities of the composite materials of Cr<sub>2</sub>O<sub>3</sub>/Pt/SrTiO<sub>3</sub> and other Rh@Cr<sub>2</sub>O<sub>3</sub> (core–shell) loaded metal oxides have been previously demonstrated for the overall water splitting.<sup>21,22</sup> In this work, we demonstrate that Cr<sub>2</sub>O<sub>3</sub>/Rh/SrTiO<sub>3</sub> can be a promising dual-purpose photocatalyst that can produce H<sub>2</sub> along with TOC removal (mineralization) of aromatic pollutants in a de-aerated aqueous suspension which is considered an inappropriate condition to achieve the mineralization of organic pollutants.

Cr<sub>2</sub>O<sub>3</sub>/Rh/SrTiO<sub>3</sub> photocatalyst was prepared by step-wise photo-deposition of Rh nanoparticles on the SrTiO<sub>3</sub> surface as a core and then the Cr<sub>2</sub>O<sub>3</sub> nano-shell on the Rh core.<sup>22</sup> The loading amount of Rh and Cr<sub>2</sub>O<sub>3</sub> was 0.5 wt% and 0.75 wt%, respectively. Fig. S1 (ESI†) shows the HRTEM images of Cr<sub>2</sub>O<sub>3</sub>/Rh/SrTiO<sub>3</sub> and Rh/SrTiO<sub>3</sub> photocatalysts. Rh nanoparticles of 2–4 nm diameter were observed to be deposited on the surface of both photocatalysts and the Cr<sub>2</sub>O<sub>3</sub> shell was seen around the Rh core of the Cr<sub>2</sub>O<sub>3</sub>/Rh/SrTiO<sub>3</sub> catalyst. Rh/SrTiO<sub>3</sub> and Cr<sub>2</sub>O<sub>3</sub>/Rh/SrTiO<sub>3</sub> were compared for the photocatalytic degradation of 4-CP under de-aerated conditions as shown in Fig. 1. Cr<sub>2</sub>O<sub>3</sub>/Rh/SrTiO<sub>3</sub> exhibited a much higher activity than Rh/SrTiO<sub>3</sub> in both the removal of 4-CP and the concurrent production of chloride (Fig. 1a). The TOC removal was also highly enhanced with Cr<sub>2</sub>O<sub>3</sub>/Rh/SrTiO<sub>3</sub> (Fig. 1b). These results clearly indicate that the removal of 4-CP in the suspension of Cr<sub>2</sub>O<sub>3</sub>/Rh/SrTiO<sub>3</sub> proceeded along with the mineralization

<sup>a</sup> School of Environmental Science and Engineering, Pohang University of Science and Technology (POSTECH), Pohang, 790-784, Republic of Korea.

E-mail: [wchoi@postech.edu](mailto:wchoi@postech.edu)

<sup>b</sup> Department of Chemistry, School of Science, Tokyo Institute of Technology, 2-12-1-NE-2 Ookayama, Meguro-ku, Tokyo 152-8550, Japan

† Electronic supplementary information (ESI) available: Experimental details of the synthesis of Rh/SrTiO<sub>3</sub>, Cr<sub>2</sub>O<sub>3</sub>/Rh/SrTiO<sub>3</sub> and F-TiO<sub>2</sub>/Pt, experimental details of photocatalytic reaction and photoelectrochemical tests, and Fig. S1–S7. See DOI: 10.1039/c6cc04260k



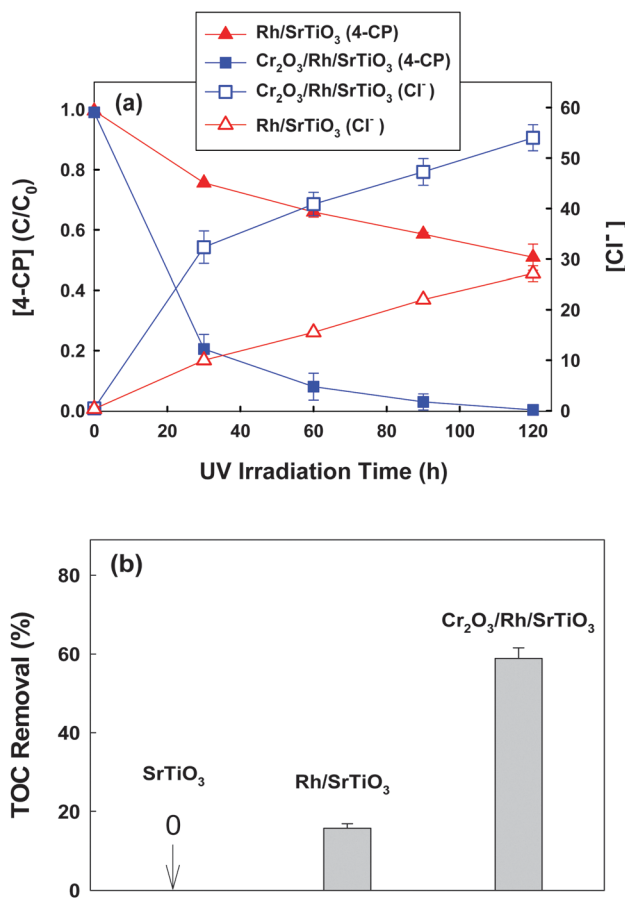


Fig. 1 (a) Photocatalytic degradation of 4-CP and the concurrent production of chloride in a de-aerated catalyst suspension. (b) Comparison of TOC removal efficiencies after 2 h photocatalytic reaction. Experimental conditions:  $[\text{catalyst}] = 0.5 \text{ g L}^{-1}$ ,  $[4\text{-CP}]_0 = 100 \mu\text{M}$ ,  $\text{pH}_0 = 7$ ,  $\lambda > 320 \text{ nm}$ , air-tight, and initially Ar-purged for 1 h before UV irradiation.

(i.e., TOC removal) even under the de-aerated conditions, where the initial dissolved  $\text{O}_2$  was measured to be less than 0.1 ppm using a dissolved  $\text{O}_2$  meter. In the absence of  $\text{O}_2$  that serves as a main electron scavenger, the photocatalytic oxidation and mineralization should be inhibited on a bare semiconductor but the loading of Rh and  $\text{Cr}_2\text{O}_3$  changes the photocatalytic reaction mechanism.

$\text{H}_2$  evolution was also monitored during the anoxic degradation of 4-CP. As seen in Fig. 2a, markedly increased  $\text{H}_2$  production was observed with the  $\text{Cr}_2\text{O}_3/\text{Rh/SrTiO}_3$  photocatalyst compared with  $\text{Rh/SrTiO}_3$ . The initial rate of  $\text{H}_2$  production on  $\text{Cr}_2\text{O}_3/\text{Rh/SrTiO}_3$  was around  $12 \mu\text{mol h}^{-1}$ . The apparent photonic efficiency of  $\text{H}_2$  evolution (with  $300 \mu\text{M}$  4-CP) was separately measured under the irradiation centered around  $\lambda = 330 \pm 10 \text{ nm}$  and determined to be 0.7%. Concurrent  $\text{O}_2$  evolution was also observed in the case of  $\text{Cr}_2\text{O}_3/\text{Rh/SrTiO}_3$ , whereas no  $\text{O}_2$  production was observed with  $\text{Rh/SrTiO}_3$ . Such a difference can be ascribed to the fact that the  $\text{Cr}_2\text{O}_3$  layer over Rh can suppress the back reaction of  $\text{H}_2$  with  $\text{O}_2$  to produce  $\text{H}_2\text{O}$ .<sup>23</sup> The fact that  $\text{O}_2$  was evolved along with the degradation of 4-CP on  $\text{Cr}_2\text{O}_3/\text{Rh/SrTiO}_3$  indicates that holes react with both 4-CP and water molecules. The *in situ* generated  $\text{O}_2$  should be subsequently consumed during the

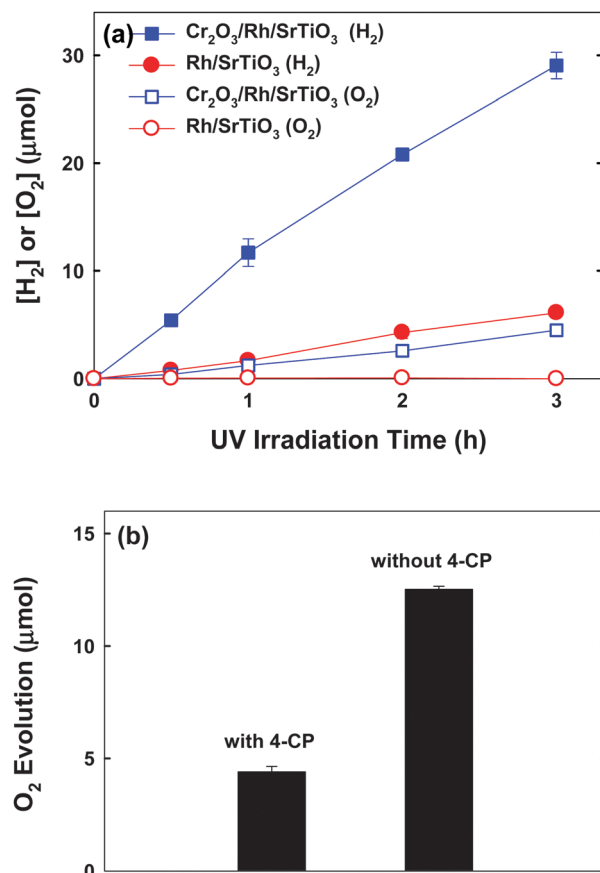
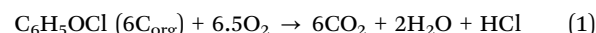


Fig. 2 (a) Time-profiled production of  $\text{H}_2$  and  $\text{O}_2$  in the suspension of  $\text{Cr}_2\text{O}_3/\text{Rh/SrTiO}_3$  and  $\text{Rh/SrTiO}_3$  with 4-CP ( $300 \mu\text{M}$ ) in the initially de-aerated suspension. (b) Comparison of photocatalytic  $\text{O}_2$  evolution in the suspension of  $\text{Cr}_2\text{O}_3/\text{Rh/SrTiO}_3$  (after 3 h reaction) in the presence and absence of 4-CP.

mineralization of 4-CP,<sup>19,24,25</sup> which explains why the degradation of 4-CP was possible under de-aerated conditions. As a result, the *in situ*  $\text{O}_2$  evolution was significantly enhanced in the absence of 4-CP (Fig. 2b). The mineralization of 4-CP can be expressed by eqn (1).



During the initial stage (for 1 h) of photo-irradiation, the rates of  $\text{H}_2$  and  $\text{O}_2$  evolution were determined to be around  $12 \mu\text{mol h}^{-1}$  and  $1.2 \mu\text{mol h}^{-1}$ , respectively. The  $\text{O}_2$  evolution rate is much lower than the expected stoichiometric rate ( $6 \mu\text{mol h}^{-1}$ ) in the dual-purpose photocatalysis, which should be ascribed to the *in situ* consumption of  $\text{O}_2$  in the mineralization (as mentioned above). In this case, the average TOC removal rate was  $5.0 \mu\text{mol h}^{-1}$ , which corresponds to  $5.4 \mu\text{mol h}^{-1}$  of the  $\text{O}_2$  consumption rate (according to eqn (1)). Therefore, the sum of the apparent  $\text{O}_2$  evolution ( $1.2 \mu\text{mol h}^{-1}$ ) and the *in situ* consumption of  $\text{O}_2$  ( $5.4 \mu\text{mol h}^{-1}$ ) is  $6.6 \mu\text{mol h}^{-1}$ , which is close to the stoichiometric  $\text{O}_2$  evolution rate of  $6.0 \mu\text{mol h}^{-1}$ . Incidentally, from a practical point of view, dual-functional photocatalysts working under air-saturated conditions would be desirable. Therefore,  $\text{H}_2$  evolution in an aerated suspension of  $\text{Cr}_2\text{O}_3/\text{Rh/SrTiO}_3$  was

also tested. As shown in Fig. S2 (ESI<sup>†</sup>), H<sub>2</sub> evolved even under air-saturated conditions although they were lower compared with Ar-saturated conditions. This result indicates that this composite photocatalyst can be effectively used for dual-functional photocatalysis in both the presence and absence of dissolved O<sub>2</sub>.

The effects of dissolved O<sub>2</sub> and the probe reagents (*i.e.*, *t*-butyl alcohol (TBA) and EDTA) were further investigated to understand the photocatalytic mechanisms of Cr<sub>2</sub>O<sub>3</sub>/Rh/SrTiO<sub>3</sub> and Rh/SrTiO<sub>3</sub>, as shown in Fig. S3 (ESI<sup>†</sup>). First, it is noted that the effects of dissolved O<sub>2</sub> are drastically different between Cr<sub>2</sub>O<sub>3</sub>/Rh/SrTiO<sub>3</sub> and Rh/SrTiO<sub>3</sub>. The presence and absence of O<sub>2</sub> did not affect the 4-CP degradation on Cr<sub>2</sub>O<sub>3</sub>/Rh/SrTiO<sub>3</sub> at all while the degradation of 4-CP on Rh/SrTiO<sub>3</sub> was significant only in the presence of O<sub>2</sub>. This observation is fully consistent with the previous reports that the Cr<sub>2</sub>O<sub>3</sub> shell layer covering the Rh core blocks the contact of O<sub>2</sub> with the Rh core, but is still permeable to protons.<sup>22,23</sup> As a result, the CB electron transfer to O<sub>2</sub> on Cr<sub>2</sub>O<sub>3</sub>/Rh/SrTiO<sub>3</sub> is insignificant but the CB electron transfer to protons (H<sup>+</sup>) is allowed with enabling the concurrent hole transfer to 4-CP. Fig. S3 (ESI<sup>†</sup>) also shows that the photocatalytic degradation of 4-CP remains unchanged in the presence of excessive TBA (as an OH radical scavenger) but is highly retarded in the presence of excessive EDTA (as a hole scavenger).<sup>26</sup> This supports that 4-CP degradation proceeds *via* a direct hole-transfer, and not an OH radical-mediated pathway.

To investigate the role of the Cr<sub>2</sub>O<sub>3</sub> shell on the Rh core and its effects on the interfacial electron transfer on Cr<sub>2</sub>O<sub>3</sub>/Rh/SrTiO<sub>3</sub> and Rh/SrTiO<sub>3</sub>, the Fe<sup>3+/2+</sup> redox couple-mediated photocurrent was collected (*via* reactions (2) and (3)) in the UV-irradiated suspension of each catalyst.<sup>27</sup>

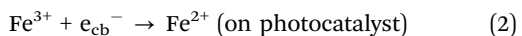


Fig. S4 (ESI<sup>†</sup>) shows that the time profile of photocurrent generation is completely suppressed by Cr<sub>2</sub>O<sub>3</sub>/Rh/SrTiO<sub>3</sub> in comparison with Rh/SrTiO<sub>3</sub>, which is the opposite to the photocatalytic activity of H<sub>2</sub> evolution. This result reconfirms that the Cr<sub>2</sub>O<sub>3</sub> layer on the Rh core suppresses the interfacial electron transfer to Fe<sup>3+</sup> ions as it hinders the electron transfer to O<sub>2</sub> molecules. The presence of the Cr<sub>2</sub>O<sub>3</sub> layer blocks the CB electron transfer to electron acceptors (*e.g.*, O<sub>2</sub>, Fe<sup>3+</sup>) except protons. On the other hand, holes generated on Cr<sub>2</sub>O<sub>3</sub>/Rh/SrTiO<sub>3</sub> are mostly consumed by water molecules with generation of O<sub>2</sub>, which enables the anoxic degradation of 4-CP. As a result, the photocatalytic production of H<sub>2</sub> on Cr<sub>2</sub>O<sub>3</sub>/Rh/SrTiO<sub>3</sub> under the de-aerated conditions depended little on the presence and kind of organic electron donors (see Fig. S5, ESI<sup>†</sup>). The photocatalytic H<sub>2</sub> production rates on Cr<sub>2</sub>O<sub>3</sub>/Rh/SrTiO<sub>3</sub> only moderately changed among the different conditions of water, 10 vol% MeOH, and 300 μM 4-CP whereas the electron donor effect on H<sub>2</sub> production was very critical for Rh/SrTiO<sub>3</sub>. This implies that the photocatalytic production of H<sub>2</sub> with the simultaneous decomposition of organic pollutants can be achieved effectively in the Cr<sub>2</sub>O<sub>3</sub>/Rh/SrTiO<sub>3</sub> photocatalytic system regardless of the kind and concentration of organic pollutants.

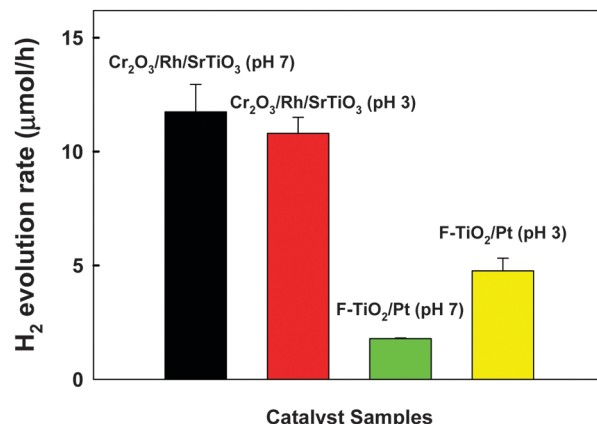
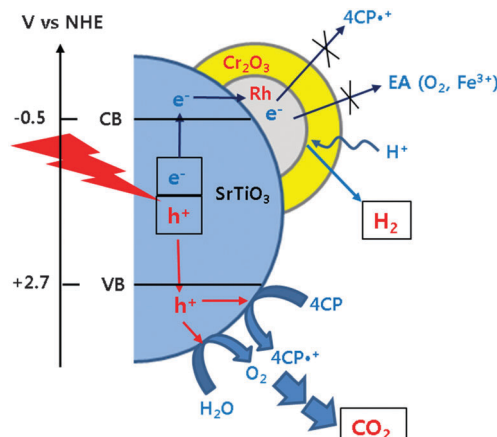


Fig. 3 Comparison of the initial photocatalytic H<sub>2</sub> production rate between Cr<sub>2</sub>O<sub>3</sub>/Rh/SrTiO<sub>3</sub> and F-TiO<sub>2</sub>/Pt photocatalytic systems in the presence of 4-CP (300 μM). Experimental conditions: [catalyst] = 0.5 g L<sup>-1</sup>,  $\lambda > 320$  nm, air-tight and initially Ar-purged for 1 h before UV irradiation.

Our recent studies demonstrated that the TiO<sub>2</sub> modified with both Pt and fluoride (F-TiO<sub>2</sub>/Pt) exhibited a dual-functional photocatalytic activity for the simultaneous production of H<sub>2</sub> and degradation of 4-CP.<sup>19,20</sup> In Fig. 3, the H<sub>2</sub> production on Cr<sub>2</sub>O<sub>3</sub>/Rh/SrTiO<sub>3</sub> was compared with F-TiO<sub>2</sub>/Pt under neutral and acidic pH conditions. The photocatalytic activity of Cr<sub>2</sub>O<sub>3</sub>/Rh/SrTiO<sub>3</sub> is higher than that of F-TiO<sub>2</sub>/Pt and less affected by the pH change. It should be noted that the activity of F-TiO<sub>2</sub>/Pt is markedly reduced at neutral pH whereas that of Cr<sub>2</sub>O<sub>3</sub>/Rh/SrTiO<sub>3</sub> was little influenced by pH. As a result, Cr<sub>2</sub>O<sub>3</sub>/Rh/SrTiO<sub>3</sub> is a better dual-functional photocatalyst from a practical point of view. In terms of the charge transfer characteristics, the following two major features make Cr<sub>2</sub>O<sub>3</sub>/Rh/SrTiO<sub>3</sub> a practical dual-functional photocatalyst. For the electron transfer part, CB electrons are selectively consumed by protons only and their transfer to O<sub>2</sub> and other electron acceptors (EA) is hindered because the Cr<sub>2</sub>O<sub>3</sub> barrier layer is selectively permeable only to protons. On the other hand, VB holes are utilized to oxidize both H<sub>2</sub>O (to O<sub>2</sub>) and 4-CP (organic pollutants) simultaneously and the *in situ* generated O<sub>2</sub> is immediately consumed for the mineralization of the organic pollutants.<sup>19,24,28</sup> The reaction mechanisms described above are schematically illustrated in Scheme 1. In the absence of the Cr<sub>2</sub>O<sub>3</sub> layer, the CB electrons can be consumed by not only protons but also *in situ* generated O<sub>2</sub> and other reaction intermediates, which would reduce the overall dual-photocatalysis activity.

To check the photostability of Cr<sub>2</sub>O<sub>3</sub>/Rh/SrTiO<sub>3</sub>, the photocatalytic H<sub>2</sub> production was repeated up to four cycles in the same batch of catalyst by injecting 100 μM 4-CP every 2 h (Fig. S6, ESI<sup>†</sup>). The activity was not maintained and gradually decreased with repeated uses. To elucidate whether the gradual loss of activity was caused by the instability of the photocatalyst, the same experiment was performed without 4-CP injection. In this case, the photocatalytic activity was maintained without showing activity loss. The composite photocatalyst itself seems to be stable. Therefore, the gradual loss of photocatalytic activity observed in the presence of 4-CP might be ascribed to



**Scheme 1** Schematic illustrations of photocatalytic reaction mechanisms occurring on the surface of  $\text{Cr}_2\text{O}_3/\text{Rh}/\text{SrTiO}_3$ .

the accumulation of organic degradation intermediates on the catalyst surface.<sup>29,30</sup> To further investigate the effect of organic compounds in this dual functional photocatalysis, the evolution of  $\text{H}_2$  and  $\text{O}_2$  was simultaneously measured with repeated photocatalysis cycles. In this case, 100  $\mu\text{M}$  4-CP was initially added but not replenished in the subsequent cycles. Fig. S7 (ESI†) shows that  $\text{H}_2$  production was higher in the first cycle than in the subsequent cycles: the difference in  $\text{H}_2$  production should be ascribed to the organic electron donor (*i.e.*, 4-CP) effect. The extra holes scavenged by 4-CP make an equal number of electrons to be used for  $\text{H}_2$  production. At the same time,  $\text{O}_2$  evolved in the first cycle is immediately consumed for the mineralization of 4-CP. As a result, the ratio of  $\text{H}_2$  to  $\text{O}_2$  in the first cycle was significantly higher ( $\text{H}_2/\text{O}_2(r) = 6.9$ ) than the stoichiometric water splitting ratio ( $r = 2.0$ ). The ratio progressively approached the stoichiometric ratio as the cycle was repeated ( $r: 6.9 \rightarrow 2.7 \rightarrow 2.5 \rightarrow 2.2$ ).

In conclusion, this study demonstrated that the mineralization of organic pollutants can be achieved under the de-aerated conditions with the simultaneous  $\text{H}_2$  production over a  $\text{Cr}_2\text{O}_3/\text{Rh}/\text{SrTiO}_3$  photocatalyst. The present study showed the highest  $\text{H}_2$  evolution efficiency in dual-purpose photocatalysis to our knowledge. It is proposed that the  $\text{Cr}_2\text{O}_3$  shell on the Rh nanoparticle core markedly enhances the  $\text{H}_2$  production and TOC removal of aromatic pollutants, which makes  $\text{Cr}_2\text{O}_3/\text{Rh}/\text{SrTiO}_3$  an active dual-functional photocatalyst.

This work was supported by the Global Research Laboratory (GRL) Program (NRF-2014K1A1A2041044), the Global Frontier R&D Program on Center for Multiscale Energy System (2011-0031571), and KCAP (Sogang Univ.) (No. 2009-0093880) funded by the Korea government (MSIP) through the National Research Foundation

of Korea (NRF). K. M. acknowledges a Grant-in-Aid for Young Scientists (A) (Project 25709078) and the PRESTO/JST program “Chemical Conversion of Light Energy” for funding support.

## References

- 1 G. Zhang, C. Ni, X. Huang, A. Welgamage, L. A. Lawton, P. K. J. Robertson and J. T. S. Irvine, *Chem. Commun.*, 2016, **52**, 1673.
- 2 M. Ni, D. Y. C. Leung and M. K. H. Leung, *Int. J. Hydrogen Energy*, 2007, **32**, 3238–3247.
- 3 F. Sastre, M. Oteri, A. Corma and H. Garcia, *Energy Environ. Sci.*, 2013, **6**, 2211.
- 4 Y. Tachibana, L. Vayssières and J. R. Durrant, *Nat. Photonics*, 2012, **6**, 511.
- 5 A. Kudo and Y. Miseki, *Chem. Soc. Rev.*, 2009, **38**, 253.
- 6 Y. Ma, X. Wang, Y. Jia, X. Chen, H. Han and C. Li, *Chem. Rev.*, 2014, **114**, 9987.
- 7 T. Hisatomi, J. Kubota and K. Domen, *Chem. Soc. Rev.*, 2014, **43**, 7520.
- 8 H. Park, Y. Park, W. Kim and W. Choi, *J. Photochem. Photobiol. C*, 2013, **15**, 1.
- 9 M. R. Hoffmann, S. T. Martin, W. Choi and D. W. Bahnemann, *Chem. Rev.*, 1995, **95**, 69.
- 10 Q. Xiang, J. Yu and M. Jaroniec, *Chem. Soc. Rev.*, 2012, **41**, 782.
- 11 J. Yang, R. Hu, W. Meng and Y. Du, *Chem. Commun.*, 2016, **52**, 2620.
- 12 H. Park, H.-i. Kim, G.-h. Moon and W. Choi, *Energy Environ. Sci.*, 2016, **9**, 411.
- 13 X.-Y. Zhang, H.-P. Li, X.-L. Cui and Y. Lin, *J. Mater. Chem.*, 2010, **20**, 2801.
- 14 M.-C. Wu, J. Hiltunen, A. Sápi, A. Avila, W. Larsson, H.-C. Liao, M. Huuhtanen, G. Tóth, A. Shechukarev, N. Laufer, Á. Kukovecz, Z. Kónya, J.-P. Mikkola, R. Keiski, W.-F. Su, Y.-F. Chen, H. Jantunen, P. M. Ajayan, R. Vajtai and K. Kordás, *ACS Nano*, 2011, **5**, 5025.
- 15 P. Gomathisankar, K. Hachisuka, H. Katsumata, T. Suzuki, K. Funasaka and S. Kaneko, *Int. J. Hydrogen Energy*, 2013, **38**, 11840.
- 16 W. Zhang, Y. Wang, Z. Wang, Z. Zhong and R. Xu, *Chem. Commun.*, 2010, **46**, 7631.
- 17 M. Wen, Y. Kuwahara, K. Mori, D. Zhang, H. Li and H. Yamashita, *J. Mater. Chem. A*, 2015, **3**, 14134.
- 18 Y.-J. Cho, H.-i. Kim, S. Lee and W. Choi, *J. Catal.*, 2015, **330**, 387.
- 19 J. Kim and W. Choi, *Energy Environ. Sci.*, 2010, **3**, 1042.
- 20 J. Kim, D. Monllor-Satoca and W. Choi, *Energy Environ. Sci.*, 2012, **5**, 7647.
- 21 K. Maeda, A. Xiong, T. Yoshinaga, T. Ikeda, N. Sakamoto, T. Hisatomi, M. Takashima, D. Lu, M. Kanehara, T. Setoyama, T. Teranishi and K. Domen, *Angew. Chem., Int. Ed.*, 2010, **49**, 4096.
- 22 K. Maeda, K. Teramura, D. Lu, N. Saito, Y. Inoue and K. Domen, *Angew. Chem., Int. Ed.*, 2006, **45**, 7806.
- 23 M. Yoshida, K. Takanabe, K. Maeda, A. Ishikawa, J. Kubota, Y. Sakata, Y. Ikezawa and K. Domen, *J. Phys. Chem. C*, 2009, **113**, 10151.
- 24 D. Hufschmidt, D. Bahnemann, J. J. Testa, C. A. Emilio and M. I. Litter, *J. Photochem. Photobiol. A*, 2002, **148**, 223.
- 25 J. Kim, J. Lee and W. Choi, *Chem. Commun.*, 2008, 756.
- 26 C. Minero, G. Mariella, V. Maurino, D. Vione and E. Pelizzetti, *Langmuir*, 2000, **16**, 8964.
- 27 H. Park and W. Choi, *J. Phys. Chem. B*, 2003, **107**, 3885.
- 28 J. Theurich, M. Lindner and D. W. Bahnemann, *Langmuir*, 1996, **12**, 6368.
- 29 M. I. Franch, J. Peral, X. Domenech and J. A. Aylón, *Chem. Commun.*, 2005, 1851.
- 30 S. Weon and W. Choi, *Environ. Sci. Technol.*, 2016, **50**, 2556.

